

# Proton Conductors : Nanometric Cavities, H<sub>2</sub> Precipitates under Pressure, and Rydberg Matter Formation

François de Guerville\*

*i2-HMR International Institute for Hydrogen Materials Research*

---

## Abstract

Proton conductors (PC) are metal oxides often used as solid electrolyte with hydrogen above 400 K, in which transmutation products and excess heat would have been obtained from near-surface locations. Near the surface of other metal oxides, closely spaced hydrogen at a distance of only 2 pm at least during a fraction of the time has been detected, and has been proposed to be in the form of hypothetical ultradense Rydberg matter H(0). How can H(0) form in PC near the cathode interface ? Nanometric cavities (NC) were observed in PC near their cathode interface. These NC would contain H<sub>2</sub> precipitates with impurities, under a pressure on the order of 0.1 GPa. Since PC are crossed by a large flux of protons, a simple mechanism is proposed to increase the H<sub>2</sub> pressure in these NC rapidly and temporarily well above the PC tensile strength. A second mechanism is then described to turn this H<sub>2</sub> into a metallic-molecular state, form a Rydberg matter H(1) and then H(0) with a pressure decrease. In NC, the presence of impurities and the entry of the hydrogen atoms in the form of Rydberg atoms are proposed to decrease the pressure required to form metallic-molecular hydrogen. Finally, different experiments are proposed to test this research approach, particularly by Transmission Electron Microscopy and Raman Micro-Spectroscopy.

**Keywords :** Proton conductors, Nanometric cavities, H<sub>2</sub> precipitates, Impurities, Large hydrogen flux, Pressure, Partial metallization of hydrogen, Rydberg states

---

## 1. Introduction

Proton conductors (PC) are mainly metal oxide crystals with perovskite structure. They can be used as solid electrolytes with H<sub>2</sub> above 400 K with porous electrodes. They are then penetrated by a very large hydrogen flux (proton conductivity up to 0.4 S/cm at 900 K) [1-3], and incorporate large concentrations of protons (several atomic %) [4].

PC are among the simplest and the most effective systems to study Condensed Matter Nuclear Science (CMNS). Mizuno *et al.* carried out CMNS experiments with polycrystalline PC based on Y-doped SrCeO<sub>3</sub> used as solid electrolytes at 650 K with deuterium passing through Pt porous electrodes, as shown in Fig. 1. Voltage and intensity were as low as 18 V and 40  $\mu$ A. The unit cell of Y-doped SrCeO<sub>3</sub> keeps a centrosymmetric structure and thus there is no additional electric polarization of the material which could give additional kinetic energy to the hydrogen ions. Transmutation products were found in the PC near their electrode interfaces [5-6], and excess heat was detected [7-9], as shown in Fig. 2. These results were confirmed by other researchers with other PC [10-12].

Holmlid and coworkers' experiments have shown that, near the surface of highly porous metal oxide crystals based on K-doped Fe<sub>2</sub>O<sub>3</sub> exposed to hydrogen, a part of the hydrogen atoms are separated from each other by only 2 pm at least during a fraction of time, as shown in Fig. 3a [13-18]. Other experiments are consistent with the presence of a significant population of compact pairs of hydrogen atoms in other hydrogenated materials [19]. This closely spaced hydrogen might be a new form of hydrogen, called H(0), shown in Fig. 3b. H(0) is a hypothetical ultradense form of Rydberg matter with a phenomenal density of 10<sup>5</sup> g/cm<sup>3</sup>. It might be a promising nuclear fuel, superfluid and superconductive at room temperature. The presence of H(0) in a PC near its cathode interface could explain the observation of transmutation products and excess heat.

H(0) would form almost spontaneously from classical hydrogen Rydberg matter H(1). H(1) can be viewed as a generalized metal [20-24]. Moreover, H(0) could be formed directly from H<sub>2</sub> at ultrahigh pressures. Thus, the route explored in this article points toward metallization of hydrogen and high pressures. The main question of this article is : How to form hydrogen Rydberg matter in a PC used as solid electrolyte with H<sub>2</sub> at 650 K near its cathode interface ?

---

\*E-mail: francois.de.guerville@i2-hmr.com

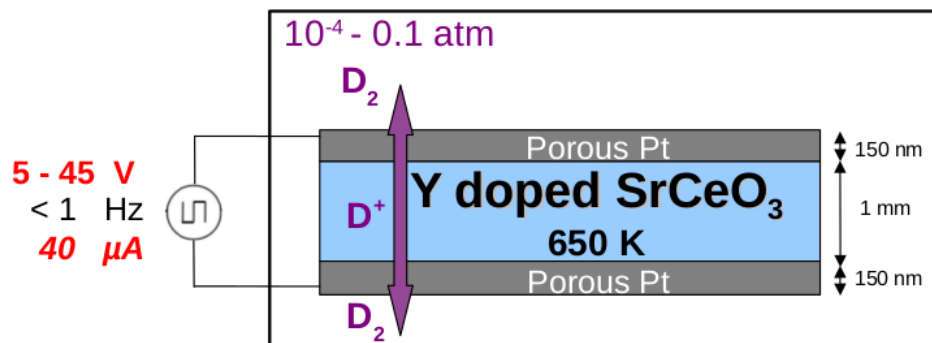


**Figure 1.** Mizuno's experimental system to study CMNS using a polycrystalline proton conductor based on Y-doped  $\text{SrCeO}_3$  as solid electrolyte with  $\text{D}_2$ . From [8].

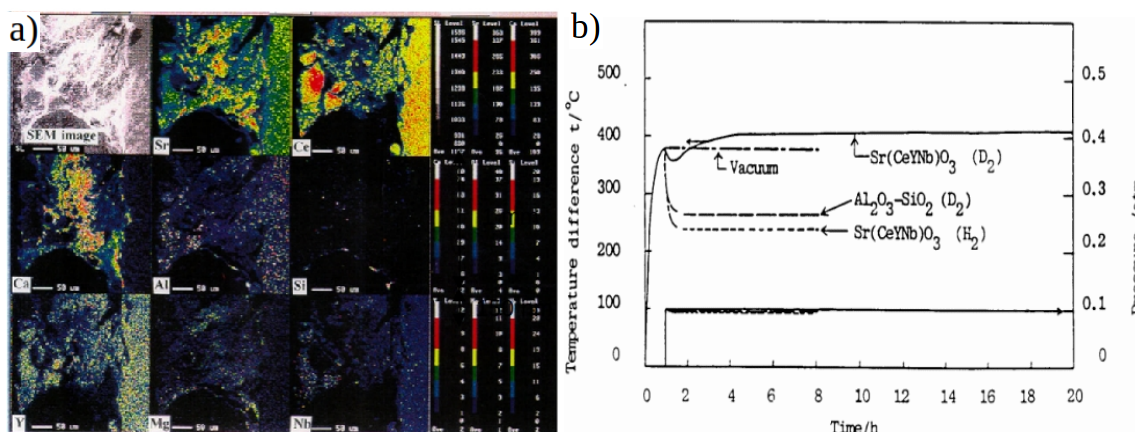


**Figure 2.** a) Transmutation products in the proton conductor Y-doped  $\text{SrCeO}_3$  near its electrode interfaces obtained with deuterium and b) excess heat. From [6] and [8].

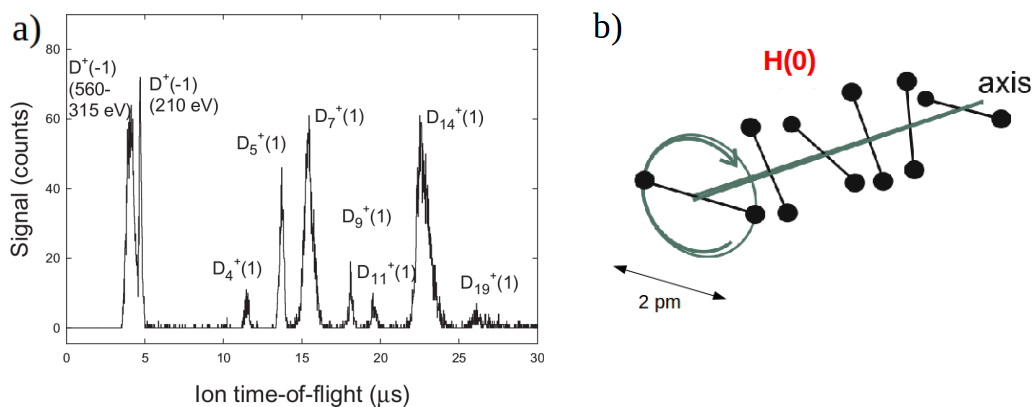


**Figure 3.** a) Closely spaced deuterons (2 pm) found near the surface of a metal oxide based on K-doped  $\text{Fe}_2\text{O}_3$ . From [13].  
b) Hypothetical ultradense hydrogen Rydberg matter  $\text{H}(0)$ . From [18].

## 2. State of the art in condensed matter physics

### 2.1. Nanometric cavities and H<sub>2</sub> precipitates under pressure

There has not been much research into nanoscale structure of PC with a large density of incorporated protons. However, crystalline silicon and metal oxides with perovskite structure implanted by large quantities of protons have been intensely studied, and this knowledge can be adapted to PC.

#### 2.1.1. In silicon implanted with H<sup>+</sup>

Silicon does not conduct protons. With the ionic implantation technique, crystal surfaces are temporarily penetrated by a large flux of hydrogen ions. This technique is used to obtain large hydrogen local concentrations in these materials, typically at a depth of roughly several hundred nanometers under the surface, as shown in Fig. 4. During material implantation, many point defects are created among which vacancy-hydrogen complexes  $V_nH_m$  [25].

During annealing, when hydrogen concentration locally overtakes the solubility limit, these mobile complexes  $V_nH_m$  agglomerate to form disk-shaped cavities of about ten nanometers in diameter [26-28]. This co-precipitation of vacancies and hydrogen, followed by the competitive growth ("Ostwald ripening") of the Nanometric Cavities (NC) and their coalescence, allow the crystalline matrix-defects system to minimize its elastic energy. Such NC are observable by Transmission Electron Microscopy (TEM) after an annealing at 720 K [26]. Figure 5a shows some NC in their disc plane (plane view). Figure 5b, obtained from a TEM cross-section of the sample, shows a NC perpendicularly to its disc plane (side view). Figure 6 shows microcracks formed from a large density of NC in the implantation zone after an annealing at 870 K [31].

These NC contain precipitates of molecular hydrogen H<sub>2</sub> [29-32]. They are traps for hydrogen and for all impurities, and they contain all the implanted hydrogen [32]. The presence of H<sub>2</sub> in these NC was established by Raman spectroscopy. In Fig. 7a, the top Raman spectrum is composed of 3 peaks. The first two correspond to Si-Si and Si-H vibrations. The third one corresponds to the H-H vibration of H<sub>2</sub> (vibron) and has a characteristic position when the H<sub>2</sub> is fluid, as it is the case here [29,30]. Figure 7b shows hydrogen molecules H<sub>2</sub> in a NC [31].

The H<sub>2</sub> filling a NC is typically pressured to a dozen of GPa at 300 K [33-36]. This value is above the tensile strength of silicon, around 7 GPa. It is expected that this internal pressure of H<sub>2</sub> is much larger during annealing above 650 K [33]. This pressure decreases when the diameter of the NC increases. Reciprocally, this H<sub>2</sub> under pressure generates stress on the crystalline matrix. The resulting strain field contrast surrounding a NC can be observed by TEM, as shown in Fig. 8a [28]. A diagram showing the pressure of H<sub>2</sub> in NC on the Si crystalline matrix is presented in Figure 8b [31].

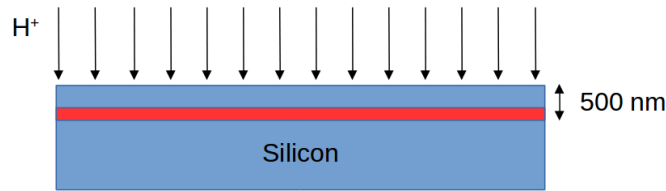


Figure 4. Ionic implantation of H<sup>+</sup> in silicon crystals.

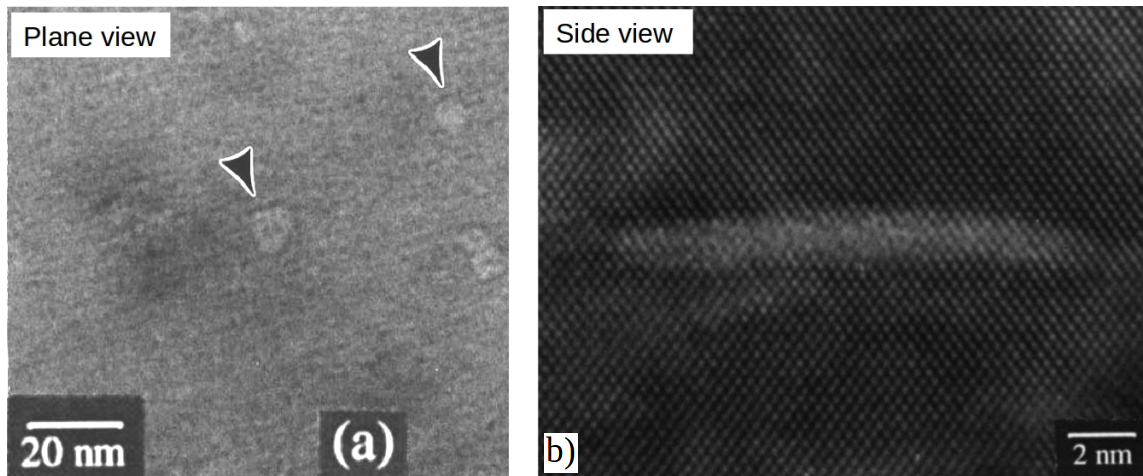
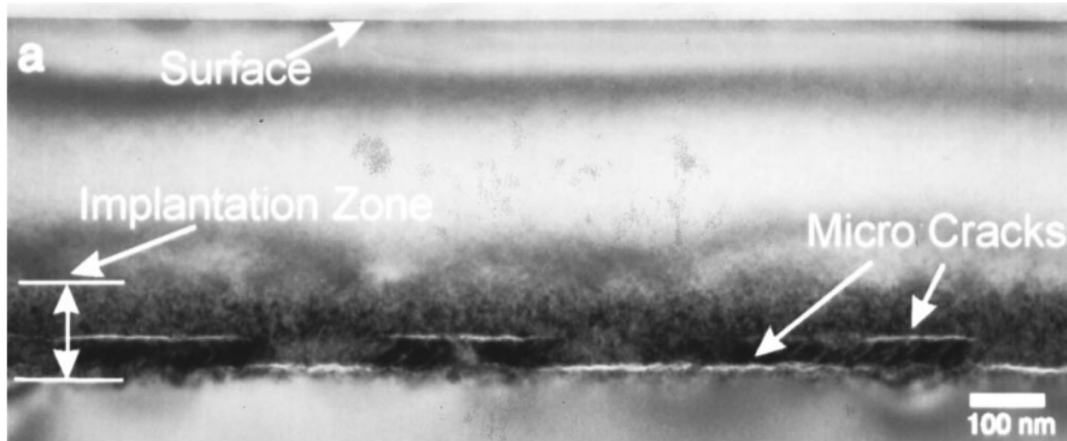
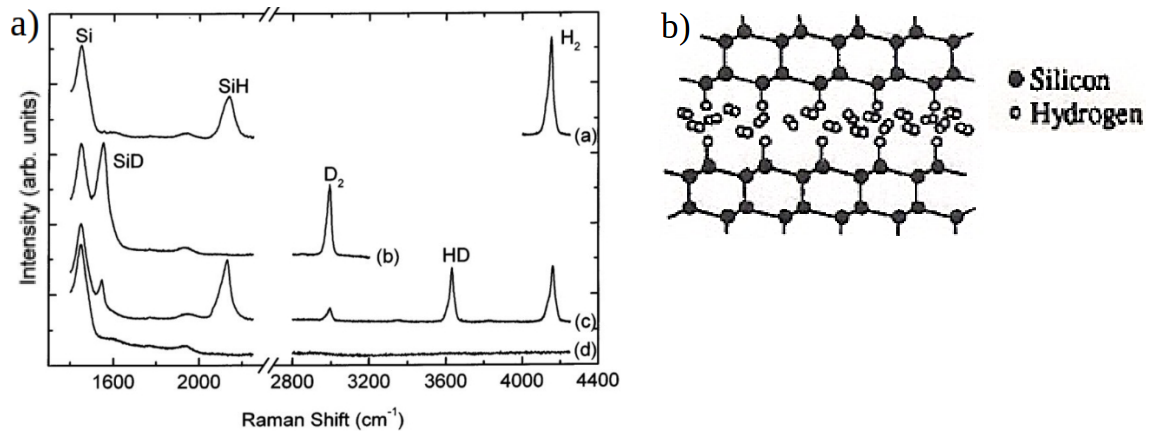


Figure 5. Nanometric cavities in H<sup>+</sup> implanted silicon, after an annealing at 720 K, observed by TEM. a) Plane view and b) cross-section side view. From [26].



**Figure 6.** Nanometric cavities in  $H^+$  implanted silicon, after an annealing at 870 K for 30 min, observed by cross-sectional TEM. From [31].



**Figure 7.** a) Raman spectroscopy on Si surface implanted with hydrogen ions at 470 K showing the presence of  $H_2$  molecules in nanometric cavities. From [30]. b) Diagram of  $H_2$  molecules trapped in Si nanometric cavities. From [31].

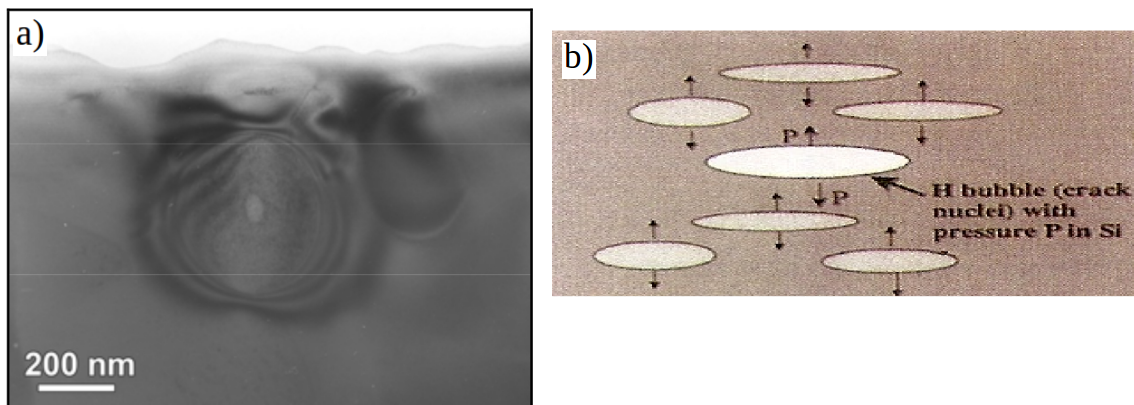


**Figure 8.** a) Cross-section TEM image showing a nanometric cavity pressurized by its internal  $H_2$ , and the long-range surrounding strain field, deep under the free surface of a hydrogenated Si wafer below 470 K. From [28]. b) Diagram showing the pressure of  $H_2$  in nanometric cavities on the Si crystalline matrix. From [31].

### 2.1.2. In metal oxides with perovskite structure implanted with $H^+$

The same phenomena are observed in metal oxides with perovskite structure, such as  $SrTiO_3$ ,  $BaTiO_3$ ,  $LaAlO_3$  and  $LiTaO_3$  [37-39]. The 2 TEM images in Fig. 9 show large densities of NC under the surfaces of  $SrTiO_3$  and  $LaAlO_3$  [37]. In hydrogen-implanted  $BaTiO_3$ , the internal pressure of  $H_2$  in microcracks was evaluated between 0.004 and 0.5 GPa [38]. This pressure should be considerably higher in NC. The tensile strength of polycrystalline  $BaTiO_3$  is 0.06 GPa.

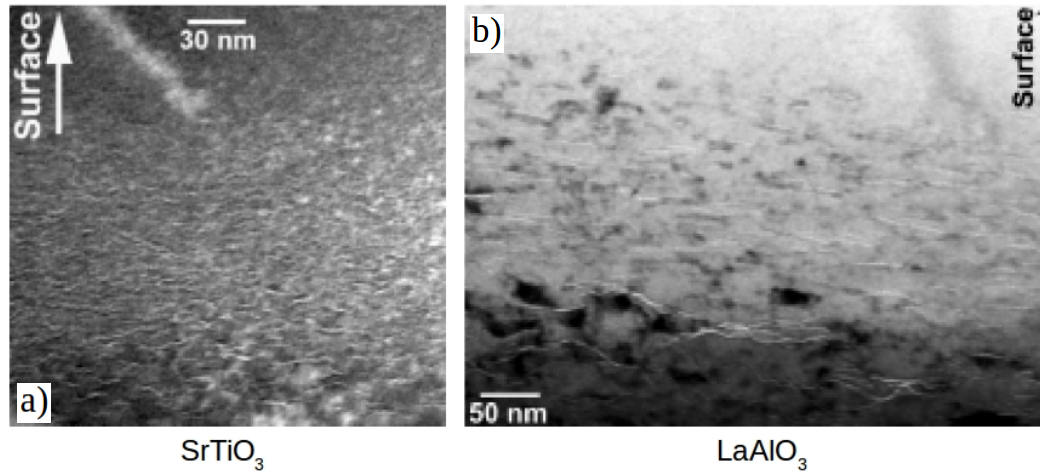


**Figure 9.** TEM images of high local densities of hydrogen related nanometric cavities (side view) in metal oxides with perovskite structure near their surfaces. These samples were implanted with hydrogen at 300 K for  $SrTiO_3$  (a) and 570 K for  $LaAlO_3$  (b). From [37].

### 2.1.3. In proton conductors used as solid electrolyte with hydrogen

High densities of NC related to hydrogen incorporation have been observed by TEM in 2 polycrystalline PC used as solid electrolyte with hydrogen [40,41]. Figure 10 shows TEM images of Gd-doped  $BaCeO_3$  used below 770 K (Fig. 10a) and Y-doped  $BaZrO_3$  used at 590 K (Fig. 10b). At least for Y-doped  $BaZrO_3$ , these NC are located within a depth of 100 nm from its cathode interface, and are oriented in parallel to it.

The phenomena observed in PC near their cathode interface when they are used as solid electrolyte with hydrogen at around 650 K can be similar to those observed in silicon and in metal oxides with perovskite structure implanted with  $H^+$ .

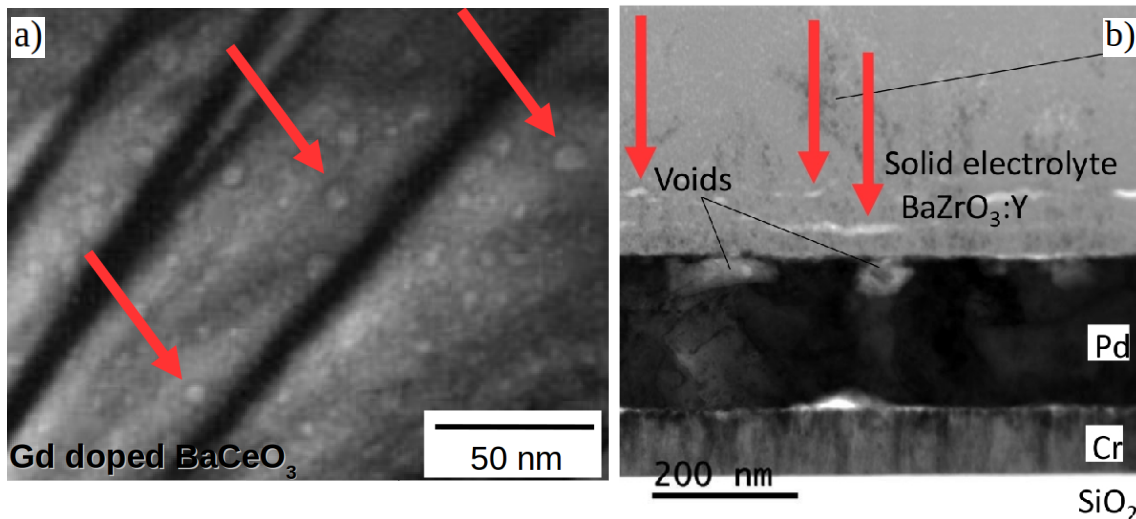


**Figure 10.** TEM images of nanometric cavities in polycrystalline proton conductors. Red arrows highlight some nanometric cavities. a) Plane view in Gd-doped  $BaCeO_3$  used below 770 K. From [40]. b) Cross-section side view in Y-doped  $BaZrO_3$  used at 590 K. From [41].

## 2.2. Partial metallization of hydrogen

### 2.2.1. Hydrogen with impurities under high pressures

Pure hydrogen can be compressed to high pressures in disk-shaped diamond anvil cells, whose dimensions are typically 100  $\mu\text{m}$  in diameter and 5  $\mu\text{m}$  in thickness [42-49]. The Pressure-Temperature phase diagram of hydrogen, obtained by Raman Spectroscopy, is presented in Fig. 11a [46-48]. Hydrogen is a molecular solid in phase I above 5 GPa at 300 K, and above 23 GPa at 650 K. Above 250 GPa at 650 K, the phase of hydrogen has not been studied yet.

Above 250 GPa and at 300 K, hydrogen is a metallic-molecular solid in phase IV and/or V. As shown in Fig. 11b, the structures of these phases are constituted of alternating layers of :

- i)  $\text{H}_2$  molecules forming sheets of graphene type by intermolecular coupling, and whose state is intermediate between metallic state and molecular state
- ii) normal hydrogen molecules  $\text{H}_2$ .

In metallic-molecular  $\text{H}_2$ , intramolecular length of  $\text{H}_2$ , initially equal to 74 pm, increases with pressure [46].

Although whether it is possible to produce metallic hydrogen in the laboratory is still debated, at around 450 GPa and at room temperature (not shown), hydrogen is supposed to be fully metallic and superconducting.

The presence of some impurities (Li, Si, S, ...) significantly decreases the pressure required to approach a metallic state when hydrogen is compressed in a diamond anvil cell [50-53]. Figure 12 shows the structure of metallic  $\text{SiH}_4$  under 113 GPa at 300 K, but  $\text{SiH}_4$  is fully metallic above only 50 GPa [51]. In this configuration, hydrogen atoms are separated from each other by 154 pm.

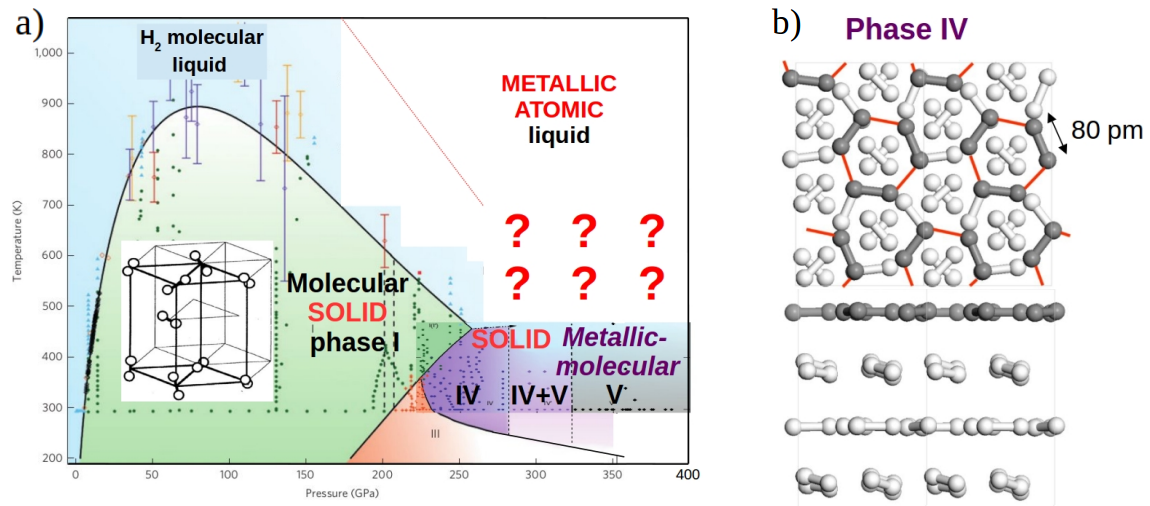


**Figure 11.** a) Phase diagram P-T of pure hydrogen, established by Raman Spectroscopy. From [42,47,48].  
b) Metallic-molecular phase IV of hydrogen. From [46].

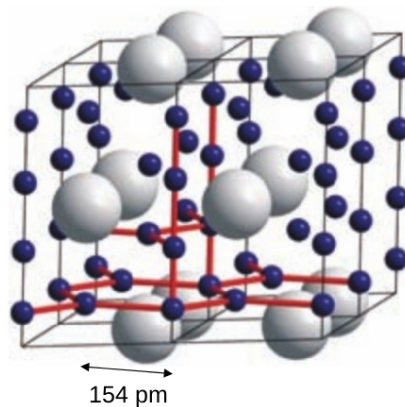


**Figure 12.** Fully metallic phase of  $\text{SiH}_4$  at only 113 GPa at 300 K. From [51].

### 2.2.2. Rydberg states

Different Rydberg states are shown in Fig. 13. A hydrogen Rydberg atom (Fig. 13a) is a hydrogen atom with its electron orbiting very far from the proton ( $> 5$  nm), quasi-circularly [54]. It results from recombination of a proton and an electron, and it easily forms on metal oxide surfaces.

Hydrogen Rydberg matter H(1) is a hexagonal plane cluster of circular Rydberg atoms (Fig. 13b), whose electrons are strongly excited and delocalized [20-24]. In this phase, hydrogen is a generalized metal which has properties similar to covalent bonding. Protons are separated from each other by 150 pm at the fundamental energy level.

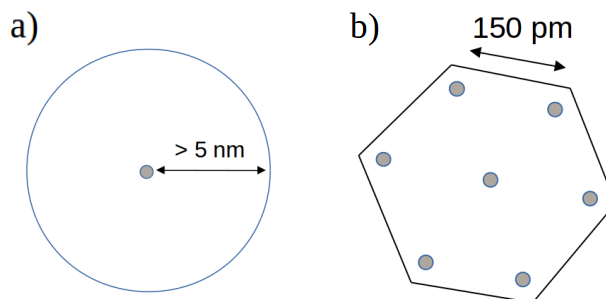


**Figure 13.** a) Hydrogen Rydberg atom. b) Hydrogen Rydberg matter H(1).

## 3. Research approach

### 3.1. Rapid and temporary increase of $H_2$ pressure in nanometric cavities of proton conductors

This research approach starts with the facts that PC, submitted to electrolysis with  $H_2$  at 650 K, can contain a high local density of NC near their cathode interface and are crossed by a large flux of hydrogen.

Hypothesis No. 1 : The NC contain  $H_2$  and hydrogen combined with impurities under a pressure on the order of 0.1 GPa.

Hypothesis No. 2 : The NC are penetrated by a large flux of hydrogen.

Hypothesis No. 3 : The entering hydrogen is trapped in the NC in the form of  $H_2$ , and the outgoing hydrogen flux is negligible compared to the entering flux.

Hypothesis No. 4 : The internal pressure of the hydrogen in the NC increases rapidly and temporary well above the PC tensile strength. The questions arising from this hypothesis are discussed in § 4.1.

### 3.2. Ultradense Rydberg matter formation in nanometric cavities of proton conductors with decrease of $H_2$ pressure

From now on, H(0) is supposed to exist and to possibly form in PC. The proposed H(0) formation mechanism is illustrated in Fig. 14.

Hypothesis No. 5 : In NC with a diameter greater than 40 nm, hydrogen penetrates in the form of circular Rydberg atoms ( $n \geq 20$ ,  $l = m = n-1$ ).

Hypothesis No. 6 : The  $H_2$  with impurities in the NC turns temporarily into a metallic-molecular phase. The required temporary internal pressure could be only on the order of tens GPa.

Hypothesis No. 7 : Circular Rydberg atoms penetrating into the NC transfer their excitation energy to the metallic-molecular sheets of  $H_2$  in the immediate proximity of the NC wall, and together, they turn into Rydberg matter H(1).

Hypothesis No. 8 : H(1) spontaneously turns into H(0) under the conditions prevailing in the NC. This transition is accompanied by a pressure decrease in the NC.

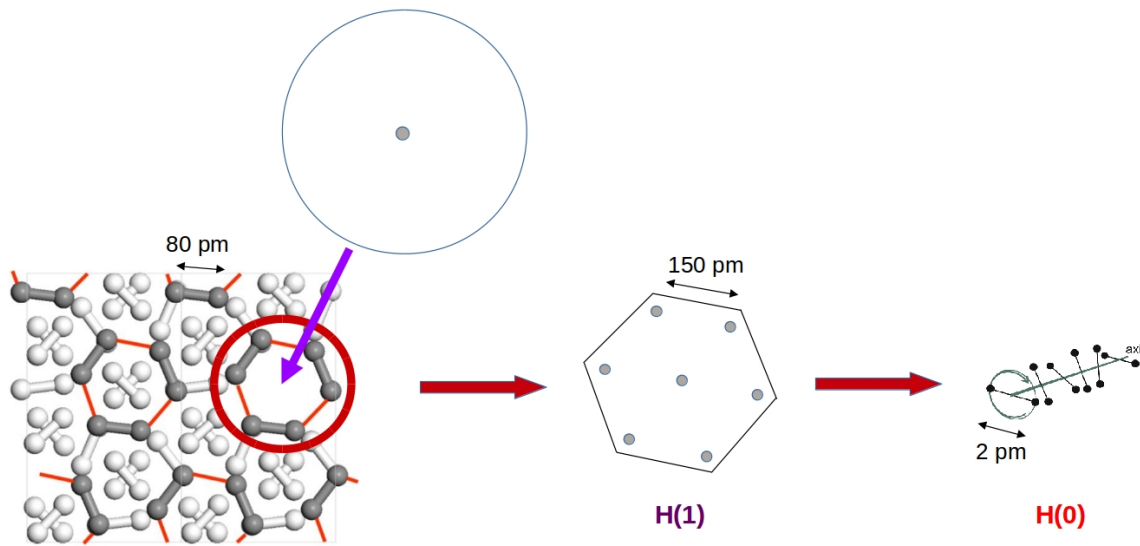


**Figure 14.** Proposed mechanism for H(1) formation in nanometric cavities consisting of circular hydrogen Rydberg atoms bombarding metallic-molecular hydrogen sheets, followed by the formation of the hypothetical H(0) and decrease of pressure.

#### 4. Discussion

##### 4.1. Rapid and temporary increase of $H_2$ pressure in nanometric cavities well above the tensile strength of the proton conductor

I have calculated that it would take 9 seconds to increase the pressure of pure hydrogen from 0.1 to 23 GPa at 650 K, in a disk-shaped NC with a thickness of 1.5 nm penetrated by a flux of 5 hydrogen atoms per  $\text{nm}^2$  per second at normal incidence, regardless of its diameter. Nowadays, better PC (for instance, Y-doped  $\text{BaZrO}_3$ ) can achieve much larger fluxes than the one considered here, estimated from [8]. Otherwise, since NC trap impurities, they might acquire a global electrical charge, and the incoming proton flux in NC might be different from what was envisaged.

In NC, what mechanisms limit this pressure increase ? From what is known for  $H^+$  implanted silicon during annealing,  $H_2$  pressure increase in NC should accelerate the NC growth by Ostwald ripening. Yet, the mechanical properties of the crystalline matrix change locally within the vicinity of a single pressurized NC [38]. Pressurized NC could implement compressive stress on the nearby PC matrix, thus having an inhibiting effect on the growth on each other [31].

Moreover,  $H_2$  pressure increase in NC should accelerate the coalescence of a tiny part of the NC into microcracks, in which the internal pressure is lower. At a given annealing temperature, depending on the local concentration of hydrogen, the characteristic time needed to form microcracks can be on the order of one hour. Consequently, the proposed rapid internal pressure increase may be little limited by the slower NC coalescence into microcracks. Finally, an open question is : Why have only Samgin *et al.* [11] reported the observation of cracks in their PC samples after CMNS experiments ?

##### 4.2. Rydberg matter formation

Other open questions follow. Is it possible to decrease the pressure required for partial metallization of hydrogen in NC down to several tens of GPa, thanks to the presence of impurities and the entry of hydrogen atoms in NC in the form of Rydberg atoms ?

What is the NC optimum size to form H(1) ? If the NC are too small, circular Rydberg atoms cannot enter them. If they are too large, the  $H_2$  internal pressure may be too low to turn  $H_2$  into metallic-molecular phase. I propose 40 nm in diameter and 1.5 nm in thickness is the optimum size. The best NC orientation should be parallel to the interfaces.

Could the formation of  $H_2$  Rydberg molecules [55] play a role in H(1) formation ?

## 5. Experimental tests to validate this approach

### 5.1. Transmission Electron Microscopy

TEM is the best tool to observe NC in a crystalline matrix, and study their locations, their sizes, their shapes, their orientations and their density.

Strain field contrast is also observable around NC containing hydrogen under pressure. Together with simulations, it is possible to deduce the  $H_2$  pressure within the NC [33].

TEM with Electron Energy-Loss Spectroscopy enables accurate mapping of hydrogen in the samples, and provides information on its bounding [56,57].

### 5.2. Raman Micro-Spectroscopy

Raman Micro-Spectroscopy reveals hydrogen vibrations and is the most adapted tool to detect the presence of  $H_2$  with impurities trapped in the NC near the cathode interface. Moreover, this technique enables us to identify and study the hydrogen phase : molecular fluid, molecular solid, metallic-molecular solid, or Rydberg matter  $H(1)$ . For  $H(1)$ , it is possible to study electronic excitation and vibrational shifts of its partially covalent bonding. However, the presence of impurities in the NC should complicate the deciphering of the Raman spectra. It may then be difficult to identify the hydrogen phase and evaluate its internal pressure.

Otherwise, stresses undergone by the crystalline matrix, generated by  $H_2$  in the NC, are also roughly assessable by Raman Spectroscopy.

Sample structural characterizations under the surface up to a depth of about 1  $\mu m$  can be carried out, after removing the cathode by chemical etching in an acid bath. By using a laser excitation wavelength below the optical absorption threshold, the probed depth can be decreased to about several hundreds of nm or less, which is the ideal depth to probe the NC. Furthermore, the use of confocal microscopy also limits the probed depth to  $\sim 500$  nm.

### 5.3. X-Ray Diffraction

X-Ray Diffraction enables to measure strain perpendicular to the surface plane in a layer of the crystalline matrix, generated by a large density of in-plane NC containing  $H_2$  under pressure. Probed depth is around 2  $\mu m$ .

### 5.4. Neutron Scattering

Neutron diffraction can detect long range ordered structure of deuterium. It does not work so well on protium, due to its lower mass. If there is enough ordered deuterium in NC, a deuterium lattice may be detectable inside.

Moreover, information could be obtained about the molecular dynamics and the collective dynamics of hydrogen (phonons) in NC.

Yet, the probed depth is very large and the bulk of the sample is probed.

### 5.5. Nuclear Magnetic Resonance Spectroscopy

A NMR spectrum with anomalously large shift in a proton NMR experiment would provide unambiguous independent confirmation of the presence of closely spaced hydrogen.

### 5.6. Laser-Induced Coulomb Explosions with Time-of-Flight Mass Spectroscopy

This technique allows to detect closely spaced hydrogen near a material surface, and evaluate the initial distance between them.

## 6. Conclusion

In proton conductors, used as solid electrolyte with hydrogen around 650 K, large densities of nanometric cavities can form near their cathode interfaces. Assuming these nanometric cavities contain  $H_2$  precipitates with impurities under a pressure on the order of 0.1 GPa, a simple mechanism is proposed to increase rapidly and temporarily the  $H_2$  internal pressure well above the tensile strength of proton conductors. Then, assuming hydrogen can exist as ultradense  $H(0)$ , a second mechanism is proposed to make the  $H_2$  with impurities in the nanometric cavities turn into a metallic-molecular phase, form Rydberg matter  $H(1)$  and then form  $H(0)$  with a pressure decrease. In NC, the presence of impurities and the entry of the hydrogen atoms in the form of Rydberg atoms are proposed to decrease the pressure required to form metallic-molecular hydrogen. Different experiments are proposed to study the hydrogen trapped in these nanometric cavities, particularly by Transmission Electron Microscopy and Raman Micro-Spectroscopy.

## References

- [1] A. Braun *et al.*, Yttrium and hydrogen superstructure and correlation of lattice expansion and proton conductivity in the  $\text{BaZr}_{0.9}\text{Y}_{0.1}\text{O}_{2.95}$  proton conductor, *Applied Physics Letters* **95** (2009) 224103.
- [2] D. Pergolesi *et al.*, High proton conduction in grain-boundary-free yttrium-doped barium zirconate films grown by pulsed laser deposition, *Nature Materials* **9** (2010) 846.
- [3] Y. B. Kim *et al.*, Effect of crystallinity on proton conductivity in yttrium-doped barium zirconate thin films, *Solid State Ionics* **198** (2011) 39.
- [4] M. Glerup *et al.*, Vibrational spectroscopy on protons and deuterons in proton conducting perovskites, *Solid State Ionics* **148** (2002) 83.
- [5] T. Mizuno *et al.*, Anomalous gamma peak evolution from SrCe solid state electrolyte charged in  $\text{D}_2$  gas, *International Journal of Hydrogen Energy* **22** (1997) 23.
- [6] T. Mizuno *et al.*, Excess heat evolution and analysis of elements for solid state electrolyte in deuterium atmosphere during applied electric field, *Journal of New Energy* **1**(1) (1996) 79.
- [7] T. Mizuno *et al.*, Anomalous heat evolution from a solid-state electrolyte under alternating current in high-temperature  $\text{D}_2$  gas, *Fusion Science and Technology* **29** (1996) 385.
- [8] T. Mizuno *et al.*, Anomalous heat evolution from SrCeO<sub>3</sub>-type proton conductors during absorption/desorption of deuterium in alternate electric field, *Proc. ICCF4* **2** (1993) 14-1.
- [9] R.A. Oriani, An investigation of anomalous thermal power generation from a proton-conducting oxide, *Fusion Science and Technology* **30** (1996) 281.
- [10] K.A. Kaliev *et al.*, Reproducible nuclear reactions during interaction of deuterium with oxide tungsten bronze, *Physics Letters A* **172** (1993) 199.
- [11] A.L. Samgin *et al.*, Cold fusion and anomalous effects in deuteron conductors during non-stationary high-temperature electrolysis, *Proc. ICCF5* **2** (1995) 201.
- [12] J-P. Bibérian *et al.*, Electrolysis of  $\text{LaAlO}_3$  single crystals and ceramics in a deuterated atmosphere, *Proc. ICCF7* (1998) 27.
- [13] S. Badiei *et al.*, Production of ultradense deuterium: A compact future fusion fuel, *Applied Physics Letters* **96** (2010) 124103.
- [14] F. Olofson *et al.*, Detection of MeV particles from ultra-dense protium p(-1): Laser-initiated self-compression from p(1), *Nuclear Instruments and Methods in Physics Research B* **278** (2012) 34.
- [15] L. Holmlid, Excitation levels in ultra-dense hydrogen p(-1) and d(-1) clusters: Structure of spin-based Rydberg matter, *International Journal of Mass Spectrometry* **352** (2013) 1.
- [16] L. Holmlid *et al.*, Meissner effect in ultra-dense protium p(l = 0, s = 2) at room temperature: superconductivity in large clusters of spin-based matter, *Journal of Cluster Science* **26** (2015) 1153.
- [17] L. Holmlid *et al.*, Spontaneous ejection of high-energy particles from ultra-dense deuterium D(0), *International Journal of Hydrogen Energy* **40** (2015) 10559.
- [18] L. Holmlid *et al.*, Phase transition temperatures of 405-725 K in superfluid ultra-dense hydrogen clusters on metal surface, *AIP Advances* **6** (2016) 045111.
- [19] J. Kasagi *et al.*, Energetic protons and  $\alpha$  particles emitted in 150-keV deuteron bombardment on deuterated Ti, *Journal of the Physical Society of Japan* **64**(3) (1995) 777.
- [20] L. Holmlid, Observation of the unidentified infrared bands in the laboratory: anti-stokes stimulated Raman spectroscopy of a Rydberg matter surface boundary layer, *The Astrophysical Journal* **548** (2001) L249.
- [21] L. Holmlid, Conditions for forming Rydberg matter: condensation of Rydberg states in the gas phase versus at surfaces, *Journal of Physics: Condensed Matter* **14** (2002) 13469.
- [22] J. Wang *et al.*, Rydberg matter clusters of hydrogen  $(\text{H}_2)_n^+$  with well defined kinetic energy release observed by neutral time-of-flight, *Chemical Physics* **277** (2002) 201.
- [23] S. Badiei *et al.*, Lowest state n = 1 of H atom Rydberg Matter: many eV energy release in Coulomb explosions, *Physics Letters A* **327** (2004) 186.
- [24] S. Badiei *et al.*, Experimental observation of an atomic hydrogen material with H - H bond distance of 150 pm suggesting metallic hydrogen, *Journal of Physics : Condensed Matter* **16** (2004) 7017.
- [25] N. Cherkashin *et al.*, Modelling of point defect complex formation and its application to  $\text{H}^+$  ion implanted silicon, *Acta Materialia* **99** (2015) 187.
- [26] J. Grisolia *et al.*, A transmission electron microscopy quantitative study of the growth kinetics of H platelets in Si, *Applied Physics Letters* **76** (2000) 852.
- [27] X. Hebras *et al.*, Comparison of platelet formation in hydrogen and helium-implanted silicon, *Nuclear Instruments and Methods in Physics Research B* **262** (2007) 24.
- [28] C. Ghika *et al.*, Hydrogen-plasma induced platelets and voids in silicon wafers, *Romanian Reports in Physics* **62** (2010) 329.
- [29] K. Murakami *et al.*, Hydrogen molecules in crystalline silicon treated with atomic hydrogen, *Physical Review Letters* **77**(15) (1996) 3161.
- [30] A. Leitch *et al.*, Formation of hydrogen molecules in crystalline silicon, *Materials Science and Engineering B* **58** (1999) 6.
- [31] T. Höchbauer *et al.*, Physical mechanism behind the ion-cut in hydrogen implanted silicon, *Journal of Applied Physics* **92** (2002) 2335.
- [32] N. Cherkashin *et al.*, Cracks and blisters formed close to a silicon wafer surface by He-H co-implantation at low energy, *Journal of Applied Physics* **118** (2015) 245301.
- [33] J. Grisolia *et al.*, TEM measurement of hydrogen pressure within a platelet, *Materials Research Society Proceedings* **681** (2001) 13.2.
- [34] X.-Q. Feng *et al.*, Mechanics of Smart-Cut(R) technology, *International Journal of Solids and Structures* **41** (2004) 4299.
- [35] B. Aspar *et al.*, Smart-Cut(R) process: an original way to obtain thin films by ion implantation, *International Conference on Ion Implantation Technology Proceedings* (2000) 255.
- [36] S. Muto *et al.*, Hydrogen-induced platelets in silicon studied by transmission electron microscopy, *Philosophical Magazine A* **72** (1995) 1057.
- [37] I. Radu *et al.*, Ferroelectric oxide single-crystalline layers by wafer bonding and hydrogen/helium implantation, *Mat. Res. Soc. Symp. Proc.* **748** (2003) U11-8-1.
- [38] Y.-B. Park *et al.*, Nanomechanical characterization of cavity growth and rupture in hydrogen-implanted single-crystal  $\text{BaTiO}_3$ , *Journal of Applied Physics* **97** (2005) 074311.

- [39] T. Luo *et al.*, IR observation on O-D vibration in LiNbO<sub>3</sub> and LiTaO<sub>3</sub> single crystal irradiated by 3 keV D<sub>2</sub><sup>+</sup>, *Journal of Nuclear Materials* **382** (2008) 46.
- [40] S.M. Haile *et al.*, The role of microstructure and processing on the proton conducting properties of gadolinium-doped barium cerate, *Journal of Materials Research* **13** (1998) 1576.
- [41] Y. Fukada *et al.*, In situ X-ray diffraction study of crystal structure of Pd during hydrogen isotope loading by solid-state electrolysis at moderate temperature, *Journal of Alloys and Compounds* **647** (2015) 221.
- [42] H.-K. Mao *et al.*, Ultra-high pressure transitions in solid hydrogen, *Review of Modern Physics* **66** (1994) 671.
- [43] M.I. Eremets *et al.*, Conductive dense hydrogen, *Nature Materials* **10** (2011) 927.
- [44] I.I. Naumov *et al.*, Graphene physics and insulator-metal transition in compressed hydrogen, *Arxiv* (2013) 1305.4649v1.
- [45] C.-S. Zha *et al.*, Raman measurements of phase transitions in dense solid hydrogen and deuterium to 325 GPa, *Proc. National Academy of Science of the U.S.A.* **111** (2014) 4792.
- [46] C.J. Pickard *et al.*, Density functional theory study of phase IV of solid hydrogen, *Arxiv* (2014) 1204.3304v2.
- [47] R.T. Howie *et al.*, Raman spectroscopy of hot hydrogen above 200 GPa, *Nature Materials* **14** (2015) 495.
- [48] P. Dalladay-Simpson *et al.*, Evidence for a new phase of dense hydrogen above 325 gigapascals, *Nature* **529** (2016) 63.
- [49] Knudson *et al.*, Direct observation of an abrupt insulator-to-metal transition in dense liquid deuterium, *Science* **348** (2015) 1455.
- [50] A.E. Carlsson *et al.*, Approaches for reducing the insulator-metal transition pressure in hydrogen, *Physical Review Letters* **50** (1983) 1305.
- [51] M.I. Eremets *et al.*, Superconductivity in hydrogen dominant materials: Silane, *Science* **319** (2008) 1506.
- [52] Y. Xie *et al.*, Superconductivity of lithium-doped hydrogen under high pressure, *Acta Crystallographica C* **70** (2014) 104.
- [53] A.P. Drozdov *et al.*, Conventional superconductivity at 203 K at high pressures, *Arxiv* (2015) 1506.08190.
- [54] T.F. Gallagher, Rydberg atoms, *Cambridge University Press, Cambridge* (1994).
- [55] J. Wang *et al.*, Formation of long-lived Rydberg states of H<sub>2</sub> at K impregnated surfaces, *Chemical Physics* **261** (2000) 481.
- [56] S. Muto *et al.*, Cross sectional TEM observation of gas-ion-irradiation induced surface blisters and their precursors in SiC, *Materials Transactions* **41** (2003) 2599.
- [57] H. Cohen *et al.*, Hydrogen analysis by ultra-high energy resolution EELS, *Microscopy and Microanalysis* **21** (2015) 661.